Available online at www.sciencedirect.com
ScienceDirect
Applied Surface Science 253 (2007) 9061–9066
applied surface science
www.elsevier.com/locate/apsusc

Corrosion behavior of boride layers evaluated by the EIS technique

I. Campos [a,*], M. Palomar-Pardavé [b], A. Amador [c], C. VillaVelázquez [a], J. Hadad [c]

[a] Instituto Politécnico Nacional. SEPI-ESIME U.P. Adolfo López Mateos, Zacatenco, Mexico D.F. 07738, Mexico
[b] Universidad Autónoma Metropolitana-Azcapotzalco, Materials Department, Avenue San Pablo 180 Col. Reynosa Tamaulipas, Mexico D.F. 02200, Mexico
[c] Tecnológico de Monterrey, Campus Ciudad de Mexico, Calle del Puente 222 Col. Ejidos de Huipulco, Mexico D.F. 14380, Mexico

Received 29 January 2007; received in revised form 8 May 2007; accepted 9 May 2007
Available online 17 May 2007

Abstract

The corrosion behavior of boride layers at the AISI 304 steel surface is evaluated in the present study. Electrochemical impedance spectroscopy (EIS) technique was used for the evaluation of the polarization resistance at the steel surface, with the aid of AUTOLAB potentiostat. Samples were treated with boron paste thickness of 4 and 5 mm, in the range of temperatures $1123 \leq T \leq 1273$ K and exposed time of 4 and 6 h. The electrochemical technique employed 10 mV AC with a frequency scan range from 8 kHz to 3 mHz in deaerated 0.1 M NaCl solution. Nyquist diagrams show that the highest values of corrosion resistance are present in the samples borided at the temperature of 1273 K, with treatment time of 4 h and 4 mm of boron paste thickness. The values of corrosion resistance on borided steels are compared with the porosity exhibited in the layers.
© 2007 Published by Elsevier B.V.

Keywords: Boriding; EIS technique; Boride layers; Polarization resistance; Borided stainless steel

1. Introduction

Boriding is the surface boron saturation of metals and alloys forming, with the base material, a surface layer consisting of one or more several inter-metallic phases. These borides are characterized by their extreme hardness and favorable wear and corrosion properties. The treatment temperatures are between 1123 and 1273 K and depending on the layer thickness required by the process, the treatment could vary from ten minutes to several hours [1–3].

Compared to powder boriding, paste boriding allows high work volumes, having as an advantage, the use of paste for selective boriding processes [4]. The control of boron paste thicknesses in this process (in the range of 3–5 mm) can generate layers thicknesses from 30 to 200 μm (taking into account the influence of time and temperature), particularly in ARMCO iron and medium and low carbon steels [5–7]. The corrosion resistance of boride-coated steels greatly depended on the amount of porosity and microcracking in the coating. A porous or cracked coating permits the penetration of corrosive media to the base material, which could cause rapid corrosion damage if the base material is not inherently corrosion resistant [8]. In the past, few studies examined the corrosion behavior of borided low and high alloy steels [9–11]. In these studies, the corrosion resistance of diverse borided steels was evaluated in several acid solutions (HCl, H_2SO_4, and H_3PO_4) for different exposure periods using two different methods: the potentiodynamic polarization experiments and the inmersion corrosion tests. The results showed that the higher corrosion resistance of the coating (FeB + Fe_2B) was observed in HCl solution while its lower corrosion resistance took place in HNO_3 solution.

This study evaluates the corrosion resistance of boride layers formed at the surface of the AISI 304 paste borided steels. The analysis employs the electrochemical impedance spectroscopy (EIS) technique. The EIS technique is usually measured by an AC potential within an electrochemical cell and establishes the current through the cell. This AC current signal contains an excitation frequency, its harmonics, and can be analyzed as a sum of sinusoidal functions (Fourier series).

2. Equivalent circuit model

The real world contains circuit elements that exhibit extremely complex behavior. These elements force the use

* Corresponding author. Tel.: +52 55 57296000x54768.
E-mail address: icampos@ipn.mx (I. Campos).

0169-4332/$ – see front matter © 2007 Published by Elsevier B.V.
doi:10.1016/j.apsusc.2007.05.016

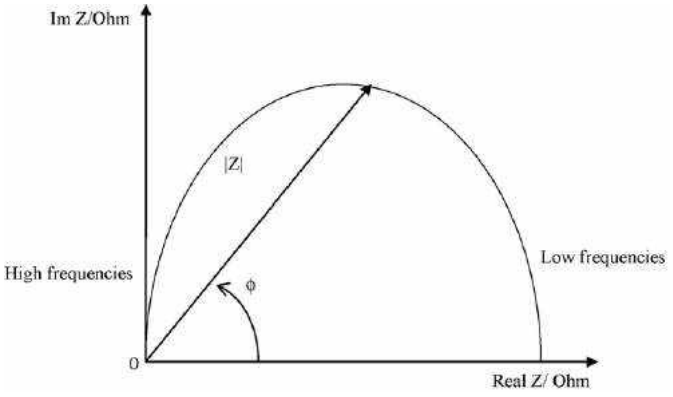

Fig. 1. Nyquist Diagram.

of impedance, which is a more general circuit parameter. Like the physical meaning of resistance, impedance is a measure of the ability of a circuit to resist the flow of electrical current. Electrochemical impedance is normally measured using a small excitation signal. The response of the system (that contains the electrochemical cell) is pseudo-linear. In a pseudo-linear system, the current corresponds to a sinusoidal potential at the same frequency. The excitation signal, expressed as a function of time, has the form:

$$E(t) = E_o \cos wt \tag{1}$$

E(t) is the potential at time t, E_o is the amplitude of the signal, and ω is the radial frequency. In a linear system, the response signal, $I(t)$, is shifted in phase (ϕ) and has a different amplitude, I_o:

$$I(t) = I_o \cos(wt - \phi) \tag{2}$$

An analogous expression to Ohm's law describes the impedance (Z) of the system as:

$$Z = \frac{E(t)}{I(t)} = Z_o \frac{\cos wt}{\cos(wt - \phi)} \tag{3}$$

On the other hand, it is possible to express the impedance as a complex function [12]. The potential is described as:

$$E(t) = E_o \exp jwt \tag{4}$$

where j represents the imaginary unit.

Then, the current response is described by:

$$I(t) = I_o \exp(jwt - j\phi) \tag{5}$$

The impedance is then represented as a complex number:

$$Z = \frac{E}{I} = Z_o \exp(j\phi) = Z_o (\cos\phi + j \sin\phi) \tag{6}$$

Eq. (6) is formed by imaginary units and real numbers represented by the Nyquist diagram (Fig. 1). The ordinate is the imaginary part while the abscissa shows the real part of the total impedance [13]. Each point in the Nyquist diagram represents the impedance obtained at each frequency.

3. Experimental procedure

3.1. Paste boriding process

The treatment was applied to AISI 304 steels cylindrical samples with a 19 mm diameter and length of 27 mm. Therefore, the samples were placed into acrylic moulds, so that the free space between the sample and the mould could be filled with boron paste. This free space could have a 4 or 5 mm thickness. The covered samples were placed into a conventional furnace under an inert atmosphere of purity argon, to sinter the paste allowing the boron diffusion into the steel substrate. The treatment temperatures were 1123, 1173, 1223, and 1273 K and two exposure times (4 and 6 h) for every boron paste thicknesses. Finally, the samples were quenched in oil, cross-sectioned and prepared for the metallographic examination and for corrosion tests. An Olympus GX51 clear-field optical microscope was used to evaluate the thickness of the borided layers. The presence of borides formed in the borided layer at the surface of the AISI 304 steel were determined by XRD analysis, using Co Kα radiation with λ = 1.54 A (Fig. 2).

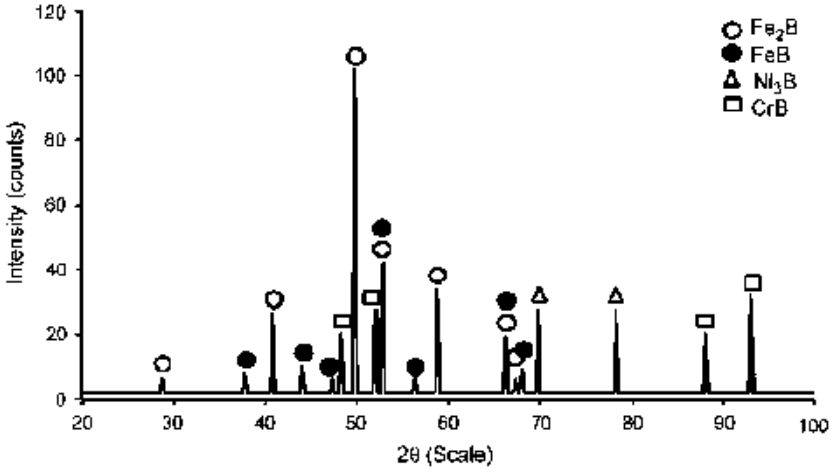

Fig. 2. XRD pattern at the surface of the AISI 304 borided steel. Temperature of 1223 K with 6 h of treatment time.

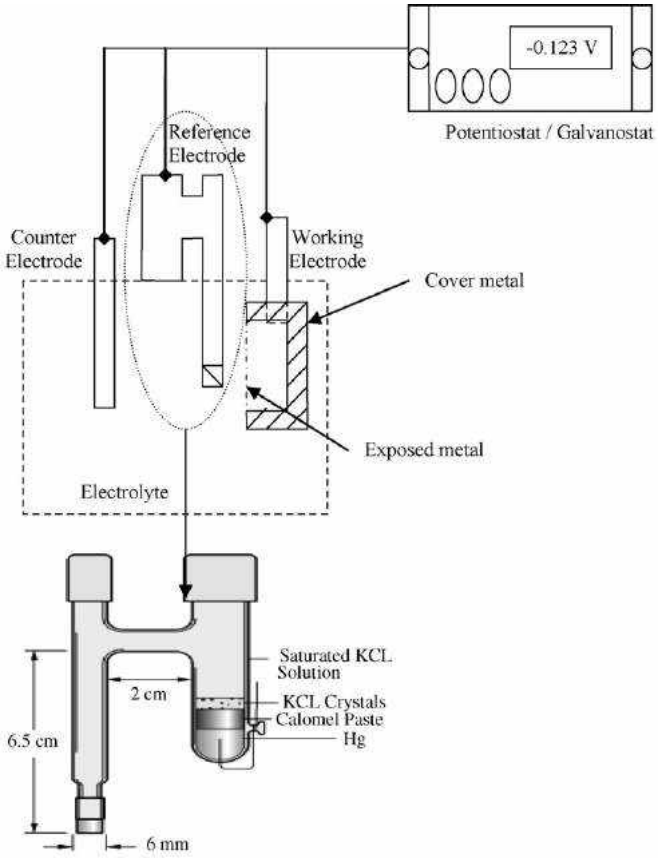

Fig. 3. Experimental setup of EIS corrosion test.

3.2. Electrochemical assays

The EIS assays were developed by means of an AUTOLAB C100 potentiostat. The borided samples were covered with an epoxy resin in order to isolate them from the electrolyte (deaerated 0.1 M NaCl solution) and leaving a free testing area of 0.0001 m^2. Five samples for each set of experimental parameters were exposed to the EIS tests, and confronted with uncoated AISI 304 steels. A hole of 3.1 mm was made along the samples, thus it was possible to make an electric union between the potentiostat and the work electrode. The working electrode consists of coating specimen, the reference electrode was a calomel-saturated electrode and a graphite bar was used as the counter electrode [14]. The experimental scheme of the electrochemical assay is shown in Fig. 3. Also, the experimental parameters of the EIS assays are given in Table 1.

4. Results and discussion

The growth of boride layers is influenced by the experimental parameters in the paste boriding process. For the temperature of 1123 K, the micrographs of borided layers reveal, considering the different values of boron paste thickness and treatment time, the presence only of the Fe_2B phase at the surface of the substrate (Fig. 4(a) and (b)). The mean value of boride layer thickness at this temperature is $\approx 9.4 \pm 3.0$. Therefore, increasing the temperature of the process, the presence of polyphase boride coatings, shown in Fig. 4(c) and (d), is visible at the surface of the AISI 304 steels. Specifically, the mean values of FeB layer thickness are from 7.5 ± 0.7 to 15.2 ± 3.5 μm, and between 13 ± 1.0 and 34 ± 3 μm for Fe_2B phase, in the boriding temperatures of 1173–1273 K and for the time process employed, respectively. The growth front is flat, due to the chemical composition of the substrate. The influence of alloying elements on the steel such as nickel and chromium produces a high surface tension at the layer/substrate interphase, as a consequence, this influence diminishes the saw-toothed morphology commonly found in layers of low-alloying carbon steels [15–17]. The influence of alloying elements on boride layer thicknesses can be explained considering that while chromium easily dissolves into iron borides depleting the underlying base alloy, nickel displays a much lower tendency to dissolve in iron borides and, therefore, concentrates beneath the boride coatings. In fact, the atomic radii of Cr and Ni are about the same and larger than that of Fe, and it can then be expected that Cr and Ni dissolved on the Fe sublattice of the borides and form solid solutions like (Fe, Cr)B, $(Fe, Cr)_2B$, (Fe, Ni)B and $(Fe, Ni)_2B$ (see Fig. 2). S. Taktak [18] showed the presence of these multicomponent borided phases by XRD patterns in AISI 304 stainless steel.

Table 1
Experimental parameters used in the EIS technique

Initial frequency (Hz)	Final frecuency (Hz)	Signal amplitude (mV)	Open circuit polarization time (s)	Number of points
8000	0.003	10	15	30

Table 2
Polarization resistance of borided steels with respect to uncoated AISI 304 steels

Boron paste thickness (mm)	Time (h)	Polarization resistance of the coating-substrate (Ω/cm^2)				Polarization resistance of uncoated AISI 304 steel (Ω/cm^2)
		1123 K	1173 K	1223 K	1273 K	770 ± 140
4	4	1500 ± 300	3800 ± 1200	6600 ± 2000	12700 ± 3200	
4	6	1400 ± 280	3800 ± 1300	2960 ± 940	5800 ± 1900	
5	4	2670 ± 350	2850 ± 820	6100 ± 1900	4300 ± 1500	
5	6	1270 ± 170	2090 ± 680	4400 ± 1400	3700 ± 1200	

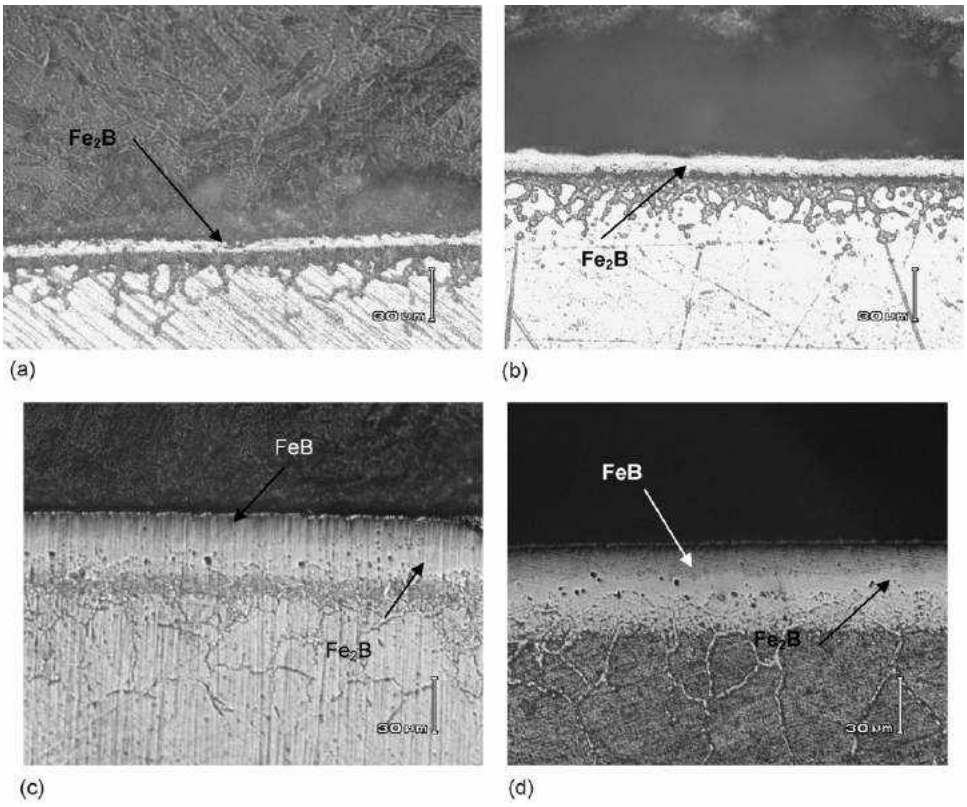

Fig. 4. Cross-sectional views of AISI 304 borided steels considering two different treatment temperatures: (a) 1123 K, 4 h and 4 mm of boron paste thickness, (b) 1123 K, 6 h and 4 mm of boron paste thickness, (c) 1223 K, 4 h and 4 mm of boron paste thickness, (d) 1223 K, 6 h and 4 mm of boron paste thickness.

Table 3
Comparison of the values for corrosion rate in borided layers obtained for different environments

Corrosion rate (gr/cm^2/day)	Type of borided steel	Environment	Reference
0.66×10^{-3}	Low carbon	HCl	[10]
1.13×10^{-3}		H_2SO_4	
3.37×10^{-3}		H_3PO_4	
1.59×10^{-3}		$HClO_4$	
0.3		HNO_3	
3.52×10^{-3}	High alloy steel (H13)	HCl	[9]
1.92×10^{-2}		H_2SO_4	
1.89×10^{-3} (mean value for all the experimental data)	304 steel	NaCl	Present work

The EIS assay gives a simple way for evaluating the corrosion resistance of the boride layers. Under this electrochemical technique, it is possible to obtain data related to the electrolyte resistance and the capacitive impedance values of the borided samples. Fig. 5 shows the Nyquist diagrams for the borided samples according to the experimental parameters of the treatment. The polarization resistance (R_p) is inversely proportional to the corrosion rate; a higher R_p, corresponds to a lower corrosion rate. R_p can be estimated from the diagram as $R_p = |Z(j\omega)|_{\omega \to 0} - |Z(j\omega)|_{\omega \to \infty}$, given that the frequency increases in a counterclockwise direction [19–20]. The solution resistance (R_s) was estimated from the impedance at high frequency ($|Z(j\omega)|_{\omega \to \infty}$), while the sum of R_p and the R_s was estimated from the impedance at low frequency ($|Z(j\omega)|_{\omega \to 0}$). The difference between these two impedance values results in R_p. The data of the borided samples show the increase of the corrosion resistance at the surface of the AISI 304 steel, compared with uncoated samples (see Table 2). The maximum corrosion resistance value was obtained with 4 h, 4 mm of boron paste thickness and 1273 K, what physically represents a compact and continuous growth of the iron boride layers with a minimum quantity of microporosities in the phases. The average value of the corrosion rate of this work[1] in AISI 304 borided steels is compared with different data obtained by other authors as shown in Table 3. The porosity is a characteristic of coatings, manifested by the existing of pores. Pores negatively affect the tightness of coatings and substantially reducing their

[1] The corrosion rates determined by electrochemical techniques are expressed in terms of current density. These expressions can be converted into penetration rates by the expression based on Faraday's law.

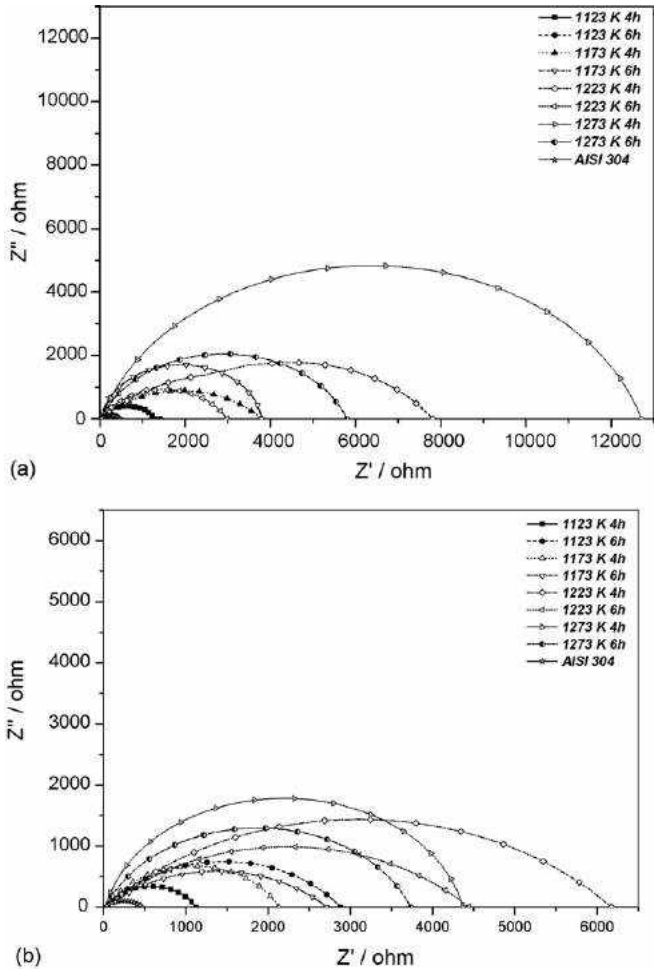

Fig. 5. Nyquist diagrams obtained by the EIS technique for the boron paste thicknesses of: (a) 4 mm and (b) 5 mm.

corrosion resistance. Porous coatings do not assure total insulation from the surrounding corrosive environment, and do not totally inhibit the diffusion of aggressive agents through the coating, which leads to the formation of local and galvanic

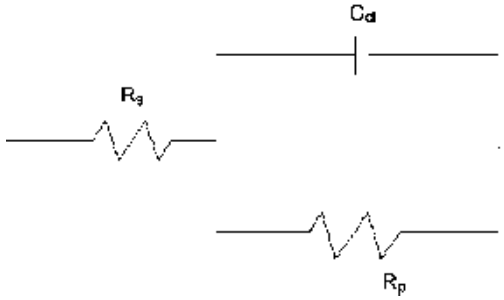

Fig. 6. Equivalent circuit proposed for the paste boriding process.

corrosion, and blistering of the coating. The porosity corresponds to the ratio of the polarization resistance for the uncoated and coated substrate [21]:

$$P = \frac{R_{p,u}}{R_{p,r-u}} \quad (7)$$

where P is the total coating porosity, $R_{p,\,u}$ is the polarization resistance of the substrate and $R_{p,\,r-u}$ is the polarization resistance of the coating-substrate system. The porosity values of borided steels are presented in Table 4. In fact, the decrease in the contact area between the borided layer and the substrate due to the porosity and the difference in the linear thermal expansion between the borides and AISI 304 steel, can carry away the exfoliation of the layer [22].

Finally, the capacitive impedance (this mean value is obtained from the Nyquist diagram) of the borided layers was determined by means of the *FRA* software along with the FRA2 module, which contains the AUTOLAB C100 potentiostat. The results are shown in Table 5. The capacitive impedance behavior can be explained by an ideal capacitor. Basically, a capacitor is formed by two plates, one against the other and separated by a small distance where a dielectric is placed. The capacitance value is directly proportional to the area of its plates and inversely proportional to the distance between them. The behavior of boride layer is similar as the plates of an ideal

Table 4
Total coating porosity of borided AISI 304 steels

Boron-paste thickness (mm)	Time (h)	Total coating porosity			
		1123 K	1173 K	1223 K	1273 K
4	4	0.51 ± 0.01	0.20 ± 0.06	0.12 ± 0.03	0.06 ± 0.01
4	6	0.55 ± 0.02	0.20 ± 0.07	0.26 ± 0.03	0.13 ± 0.04
5	4	0.28 ± 0.02	0.26 ± 0.06	0.13 ± 0.03	0.18 ± 0.06
5	6	0.60 ± 0.05	0.37 ± 0.01	0.17 ± 0.05	0.21 ± 0.06

Table 5
Capacitive impedance values of borided samples and uncoated AISI 304 steel

Boron-paste thickness (mm)	Time (h)	Mean values of capacitive impedance (μF)				Capacitive impedance of uncoated AISI 304 steel (μF)
		1123 K	1173 K	1223 K	1273 K	2623 ± 493
4	4	158 ± 30	123 ± 20	117 ± 22	110 ± 21	
4	6	159 ± 30	125 ± 25	124 ± 23	121 ± 23	
5	4	121 ± 23	113 ± 21	117 ± 22	108 ± 24	
5	6	122 ± 21	111 ± 21	113 ± 21	106 ± 22	

capacitor, with a constant area (determined as the exposed corrosion test area) and distance d, that represents the total layer thickness of borided phases. With the values of polarization resistance, capacitive impedance and the electrolyte resistance, an electrical model can be constructed: a R_S solution resistance connected in series with the R_p polarization resistance in parallel to a C_{dl} capacitor (Fig. 6).

5. Conclusions

The use of EIS technique facilitates the evaluation of the corrosion resistance of borided layers formed at the surface of AISI 304 steels. During the paste boriding process, the growth fronts of the layers are flat, due to the presence of alloying elements that inhibit the active boron flux in zones of preferential growth of iron borides. On the other hand, the borided samples present a significant increase in the corrosion resistance at the steel surface, in comparison to the non-thermochemical treated samples.

The polarization resistance behavior of boride layers is in relation with the total porosity exhibited by the phases formed at the steel surface. When the polarization resistance increases, the porosity values decreases, considering the set of experimental parameters at constant temperature. The Nyquist diagrams are also used to determining the capacitive impedance of the boride layers, whose value is inversely proportional to the layer thickness. The equivalent circuit obtained by the EIS technique consists of the solution resistance R_s of the test electrolyte between the working electrode (boride coating), whose defects are characterized by a parallel capacitor, and the reference electrode.

Acknowledgments

I. Campos thanks the project *20070130* chair supported by the *Secretaría de Investigación y Posgrado* of the Instituto Politécnico Nacional and to the research grant 53859 of the Consejo Nacional de Ciencia y Tecnología at México.

References

[1] G. Wahl, Durferrit-Technical Information. Reprint from VDI-Z117 (1975), 785–789.
[2] A. Graf von Matuschka, Boronizing, Carl Hanser Verlag, Germany, 1980
[3] A.K. Sinha, Boronizing, J. Heat Treatment 4, ASM Handbook, USA, 1991.
[4] I. Campos, O. Bautista, G. Ramírez, M. Islas, J. De la Parra, L. Zúñiga, Appl. Surf. Sci. 252 (2005) 2396–2403.
[5] E. Meléndez, I. Campos, E. Rocha, M.A. Barrón, Mater. Sci. Eng. A 234–236 (1997) 900–903.
[6] G. Palombarini, M. Carbucicchio, J. Mat. Sci. Lett. 3 (1984) 791–794.
[7] M. Carbucicchio, G. Palombarini, J. Mat. Sci. Lett. 6 (1987) 1147–1149.
[8] S.C. Singhal, Thin Solid Films 45 (1977) 321–329.
[9] G. Kariofilis, G. Kiourstsidis, D. Tsipas, Surf. Coat. Technol. 201 (2006) 19–24.
[10] G. Kartal, O. Kahvecioglu, S. Timur, Surf. Coat. Technol. 200 (2006) 3590–3593.
[11] E. Atik, U. Yunker, C. Meric, Tribol. Inter. 36 (2003) 155–161.
[12] J.R. Scully, D.C. Silverman, M.W. Kendig, Electrochemical Impedance: Analysis and Interpretation, ASTM Special Technical Publication Stp. 1, USA, 1993.
[13] J. Fontana, Corrosion Engineering, Mc Graw-Hill, USA, 1990.
[14] A.J. Bard, L.R. Faulkner, Electrochemical Methods: Fundamentals and Applications, Wiley Interscience Publications, USA, 2001.
[15] I. Campos, M. Palomar, A. Amador, R. Ganem, J. Martínez, Surf. Coat. Technol. 201 (2006) 2438–2446.
[16] C. Bindal, A. Ucisik, Surf. Coat. Technol. 122 (1999) 208–213.
[17] C. Carbucicchio, G. Sambogna, Thin Solid Films 126 (1985) 299–305.
[18] S. Taktak, Materials and Design 28 (2007) 1836–1843.
[19] A.J. Bard, L.R. Faulanker, Electrochemical Methods, Wiley Interscience Publications, USA, 1987.
[20] C.C. Lin, K.L. Chang, H.C. Shih, Appl. Surf. Sci. 253 (2007) 5011–5016.
[21] S.H. Ahn, J.H. Yoo, J.G. Kim, J.G. Han, Surf. Coat. Technol. 163–164 (2006) 611–619.
[22] J.H. Wang, J.G. Duh, H.C. Shih, Surf. Coat. Technol. 78 (1996) 248–250.